New Boundary Condition for the Two Dimensional Stationary Boussinesq Paradigm Equation

K. Angelow (angelow@math.bas.bg)

Abstract
In this paper the stationary propagating wave solution to the two dimensional Boussinesq equation is examined, which is a solution to a nonlinear fourth order elliptic equation. We propose and apply a new boundary condition (BC) on the computational boundary. The numerical algorithm for computation of stationary propagating waves is based on high order accurate finite difference schemes. The performed numerical tests confirm the validity of the new BC. A comparison with the known in the literature formulas is also given.

Key words:
stationary wave, Boussinesq equation, boundary, soliton, uniform grid, false transient method

1. Introduction

In this paper we consider stationary solutions (solutions of type $u(x,y,t)=U(x,y-ct)$) to the two dimensional Boussinesq Paradigm Equation (BE)

$$\begin{aligned} &u_{tt}-\Delta u-\beta_1\Delta u_{tt}+\beta_2\Delta^2 u+\Delta f(u)=0, \quad for\ (x,y)\in\Re^2, t\in\Re^+ \\ &u(x,y,0)=u_0(x,y), u_t(x,y,0)=u_1(x,y) \\ &u(x,y)\to 0, \Delta u(x,y)\to 0, \quad for\sqrt{x^2+y^2}\to\infty, \end{aligned} \tag{1.1}$$

where $f(u)=\alpha u^2$, $\alpha,\beta_1,\beta_2>0$ are real constants and Δ is the Laplace operator. A derivation of the BE from the original Boussinesq system with discussion on the different mechanical properties could be found e.g. in [1].

The one-dimensional (1D) BE is famous with its approximation for long waves propagating in shallow water [2], [3]. Furthermore, 1D BE admits localized wave solutions (called 'solitons'),

$$u_{tt}-u_{xx}-\beta_1 u_{xxtt}+\beta_2 u_{xxxx}+\left(u^2\right)_{xx}=0 \tag{1.2}$$

which maintain shape and emerge unchanged from collisions with other traveling waves, appear to be a very suitable model for particles, [4], [5], [6].

We try to find a stationary, traveling in *y* direction with phase velocity *c*, wave solution to the 2D BE, i.e. a solution to (1.1) of type $u(x,y,t)=U(x,y-ct)$. The waves *U* satisfy the nonlinear fourth order elliptic equation:

$$c^2(E-\beta_1\Delta)U_{yy}=\Delta U-\beta_2\Delta^2 U-\Delta f(U). \quad (1.3)$$

If the condition $c<\min\left(1/\sqrt{\beta}\ ,1\right)$, $\beta=\beta_1/\beta_2$ holds, then (1.3) is an elliptic equation of fourth order and the linear second order derivatives in (1.3) form a second order elliptic equation. In this paper we consider velocities *c* which fulfill this inequality.

The aim of this paper is to evaluate numerically the stationary soliton solution U to (1.1), i.e. the solution to (1.3). In the future, it is planned to investigate this solution as a candidate for a two dimensional 'soliton-like' solution of the nonstationary problem (1.1) (to study the evolution in time of the shape of this solution and the collision of two solutions).

Different solution techniques have been applied through the investigation of the elliptic problem (1.3). The "False Transient Method" and the "Galerkin Spectral Method" are used in [7], [10]; the "Fourier Galerkin Method" is implemented in [9], [10] and the "The Perturbation Solution" - in [11].

We emphasize that both problems, Eq. (1.1) and Eq. (1.3), are posed on unbounded domain – the plane R^2. Thus we have to limit the domain of computation numerically so that the numerical solution will approximate the exact solution for the unbounded domain and, moreover, to keep the overall computational cost reasonable.

So we have to state an artificial boundary Ω and artificial boundary conditions (BC), known in the literature as 'absorbing' boundary conditions (BC) or 'nonreflecting' BC (see [12] for a wave equation, [13] for a Helmholtz type equation, [14] for elliptic second order equation, etc.).

The problem for posing artificial BC for BE is studied in [7], where first the following asymptotic of U is found

$$U(r)\sim\frac{C_u}{r^2}, \quad \text{for } r>>1. \quad (1.4)$$

In this paper a new and more sophisticated artificial BC for stationary BE (1.3)

$$U(r)=\mu\frac{(1-c^2)x^2-y^2}{((1-c^2)x^2+y^2)^2}\Big|_{\partial\Omega} \quad (1.5)$$

is proposed. The information about the known outer solution- the solution, valid for sufficiently large *r*, $r = \sqrt{x^2 + y^2} \to \infty$, is used. This condition has an analytical form, which directly depends on the velocity *c*. Furthermore, high order finite difference schemes are used for numerical evaluation of the solution to problem (1.3). The new BC (1.5) and the numerical method are validated by performing a series of experiments, as mesh refinement and computations on different space domains. A comparison of the obtained here results with the similar results from [11] is also discussed.

2. Derivation of the new asymptotic boundary conditions

Problem (1.3) can be rewritten as a system of two elliptic equations of second order in different ways. We expect that the derivative U_{xx} in *x* direction will be smaller than the derivative U_{yy} in *y* direction because the solution moves along the y-axis. Therefore the equality $U_{yy} = \Delta U - U_{xx}$ is substituted in (1.3) and after introducing an auxiliary function *W*, we obtain an equivalent to (1.3) system of two elliptic equations:

$$\begin{aligned} &\left(1-c^2\right)U + \left(c^2\beta_1 - \beta_2\right)\Delta U - f\left(U\right) = W \\ &\Delta W = -c^2\left(E - \beta_1\Delta\right)U_{xx}. \end{aligned} \qquad (2.1)$$

We have to complete the system (2.1) with appropriate boundary conditions for functions *U* and *W*. In [7] the behavior of the solution *U(r)* for $r = \sqrt{x^2 + y^2} \to \infty$ is studied in details. From the mathematical analysis and numerical results provided there it follows that *U*(*r*) and *W*(*r*) have $O(r^{-2})$ asymptotic decay at infinity.

The main goal of this paper is to derive a new implementation of these asymptotic conditions and to use them on the boundary of a truncated computational domain Ω_h.

We would like to go further by estimating which terms in the equations (1.3) define the asymptotic behavior and then validate our proposition by numerical tests. At first, suppose that for sufficiently large *r* the second order derivatives $\Delta U, c^2 U_{yy}$ of *U* are of order $O(r^{-4})$, whereas the fourth order derivatives and the nonlinear term, i.e. $\Delta^2 U, c^2 \Delta U_{yy}, \Delta f(U)$ in equation (1.3) are of order $O(r^{-6})$.

Now consider equation (1.3) for sufficiently large values of *r*. We insert the asymptotic values of all terms in (1.3) and neglect the higher order terms of order $O(r^{-6})$ inside the *r*-expansion. Thus for large values of *r* the following formulas are valid

$$\Delta\bar{U}(x,y) = c^2\bar{U}(x,y), \qquad \bar{U}(x,y) \sim \frac{1}{x^2+y^2} \quad \text{for } x^2+y^2 \to \infty \text{ .(2.2)}$$

We apply the following change of variables

$$\bar{x} = \sqrt{1-c^2}\,x, \quad \bar{y} = y, \quad \bar{v}(\bar{x},\bar{y}) := \bar{U}(x,y) \quad (2.3)$$

and transform (2.2) into the Laplace equation for the new function $\bar{v}$

$$\Delta\bar{v} = 0, \quad \bar{v}(\bar{x},\bar{y}) \sim \frac{1}{\bar{r}^2} \quad \text{for} \quad |\bar{r}| = \sqrt{\bar{x}^2+\bar{y}^2} \to \infty. \text{ (2.4)}$$

In polar coordinates the equation (2.4) is rewritten as:

$$\frac{\partial^2}{\partial\bar{r}^2}\bar{v}(\bar{r},\theta) + \frac{1}{r}\frac{\partial}{\partial\bar{r}}\bar{v}(\bar{r},\theta) + \frac{1}{r^2}\frac{\partial^2}{\partial\theta^2}\bar{v}(\bar{r},\theta) = 0. \text{ (2.5)}$$

After the separation of variables $\bar{v}(\bar{r},\theta) = H(\bar{r})G(\theta)$ we get the following general form of functions *G* and *H*

$$\begin{aligned} H(\bar{r}) &= \sum_{n=2}^{\infty}\left(\mu_{1,n}\frac{1}{\bar{r}^n} + \mu_{2,n}\bar{r}^n\right), \\ G(\theta) &= \sum_{n=2}^{\infty}\left(\mu_{3,n}\sin(n\theta) + \mu_{4,n}\cos(n\theta)\right). \end{aligned} \qquad (2.6)$$

We fix the parameters $\mu_{2,i}, i \geq 2$ to zero because of the asymptotic limitation that $H(\bar{r}) \sim \frac{1}{\bar{r}^2}$ for $|\bar{r}| \to \infty$. For simplicity we take into account the main term in the expansion of *H(r)* and set $\mu_{1,i}, i \geq 3$ to zero. Analogously we set $\mu_{3,i}, i \geq 2$ and $\mu_{4,i}, i \geq 3$ to zero. Further artificial simplification is made by setting $\mu_{32} = 0.$

In this way we obtain the following representation of the main asymptotic term in $\bar{v}$

$$\bar{v}(\bar{r},\theta)=\mu\frac{\cos(2\theta)}{\bar{r}^2}=\mu\frac{\cos(\theta)^2-\sin(\theta)^2}{\bar{r}^2}=\mu\frac{\bar{x}^2-\bar{y}^2}{(\bar{x}^2+\bar{y}^2)^2},\quad(2.7)$$

where $\mu:=\mu_{42}\mu_{12}$. In the old (x,y) coordinate system, (2.7) reads as:

$$U(x,y)=\mu\frac{(1-c^2)x^2-y^2}{((1-c^2)x^2+y^2)^2}.\qquad(2.8)$$

We treat the second function W from (2.1) in a similar way and obtain similar asymptotical representation for W

$$W(x,y)=\hat{\mu}(1-c^2)\frac{(1-c^2)x^2-y^2}{((1-c^2)x^2+y^2)^2}.\qquad(2.9)$$

The unknown constants μ and $\hat{\mu}$ included in (2.8) and (2.9) are calculated in each iteration by the least squares fitting method using points near the boundary and on the boundary itself. In the following numerical computations we use the new BC (2.8) and (2.9) as BC on the situated far away from origin boundary of the truncated domain Ω_h.

Note that in the analytical representation of the new BC (2.8) and (2.9) the phase speed c of the wave is directly included in the equation.

3. Numerical method for the elliptic system

In order to relate to our previous results from [15] and [16], we make the following change of variables

$$\begin{aligned}&\tilde{x}=\frac{x}{\sqrt{\beta_1}},\tilde{y}=\frac{y}{\sqrt{\beta_1}},\\&\tilde{U}(\tilde{x},\tilde{y})=U(x,y),\quad\tilde{W}(\tilde{x},\tilde{y})=\beta W(x,y)\end{aligned}\qquad(3.1)$$

Then problem (2.1) is transformed into the new system of elliptic equations:

$$\begin{aligned}&(\beta-\tilde{c}^2)\tilde{U}-(1-\tilde{c}^2)\Delta\tilde{U}-\beta f(\tilde{U})=\tilde{W}\\&\Delta\tilde{W}=-\tilde{c}(E-\Delta)\tilde{U}_{\tilde{x}\tilde{x}}\end{aligned}\qquad(3.2)$$

with $\beta = \beta_1/\beta_2$ and $\tilde{c} = \sqrt{\beta}c$. The transformation (3.1) modifies the BC (2.8) and (2.9) as follows:

$$
\begin{aligned}
&U_B(\tilde{x},\tilde{y}) = \mu_U B(\tilde{x},\tilde{y}),\\
&W_B(\tilde{x},\tilde{y}) = \mu_W B(\tilde{x},\tilde{y}), \text{where}\\
&B(\tilde{x},\tilde{y}) := \frac{(1-\tilde{c}^2/\beta)\tilde{x}^2 - \tilde{y}^2}{((1-\tilde{c}^2/\beta)\tilde{x}^2 + \tilde{y}^2)^2}.
\end{aligned}
\qquad (3.3)
$$

We intend to use the solution of (1.3) as initial condition to hyperbolic problem (1.1). Therefore, an essential step for solving equations (1.1) and (1.3) is choosing the appropriate grid type. The uniform and non-uniform grids define two different investigation approaches. The meshing, that has been predominantly used in most cited papers for the numerical analysis of BE, is the non-uniform one, see e.g. [7]. It has big time advantage of generating a fast solution for the elliptic equation (1.3), but also creates a major problem when moving the solution of (1.3) in the hyperbolic equation (1.1). The ultimate goal is to develop an algorithm which investigates collision of two waves with arbitrary phase speeds *c*. Shifting the traveling waves in the hyperbolic equation on a larger distance, and further colliding two 'soliton-like' solutions requires a uniform grid. Therefore we decide to apply an uniform grid to solve the equation (1.3).

The numerical method for solving (3.2), developed in this paper, uses the false transient method from [10] and [17]. This method introduces a pseudo-time derivative and modifies the elliptic system (3.2) to a parabolic one. The stationary solution to problem (3.2) is obtained after the convergence of the solution to the parabolic problem. The initial data for the iteration process is chosen as the 'best-fit' formulas described in [11].

The uniform grid and symmetric finite differences of fourth and sixth order of approximation to second order spatial derivatives in (3.2) are applied for the discretization of the corresponding parabolic problem. Moreover, we apply the new BC (3.3) on the boundary of the computational domain $\tilde{\Omega}$.

In order to resolve the boundary functions in (3.3) completely one needs the values of μ_U and μ_W. These are obtained iteratively, at each time level of the algorithm for solving parabolic problem, by the minimization procedure described here.

For a given numerical solution $\hat{U}^k$ at the time level t_k we choose μ_U as minimizer of the problem

$$\mu_U = \min_{\mu_U > 0} \left\| U_B(\tilde{x}_i, \tilde{y}_j) - \hat{U}^k_{i,j} \right\|_{L_2, \Omega_B}, \qquad (3.4)$$

where $(\tilde{x}_i, \tilde{y}_j) \in \tilde{\Omega}$ describes the computational domain meshed with uniform grid with step *h*, and $\hat{U}_{i,j}$ is the numerical solution at the mesh point $(\tilde{x}_i, \tilde{y}_j)$. The set Ω_B includes not only the boundary nodes on $\partial\tilde{\Omega}$ but also all inner nodes lying at distance $(2h, 4h, ...)$ from the boundary $\partial\tilde{\Omega}$. The minimization problem (3.4) produces a simple linear equation with respect to μ_U.

4. Validation of the new boundary conditions

Two tests are made to verify the new BC on the boundary of the computational domain. The finite difference schemes are of fourth order of approximation and the following constants of the problem (3.2) are fixed: $\alpha = 1$, $\beta = 3$ and $\tilde{c} = 0.45$.

Test 1.

It reviews the behavior of the parameter μ_U, defined in the formula (3.3). In Table 1, for computational domains $\tilde{\Omega} = \left[-L_{\tilde{x}}, L_{\tilde{x}}\right] \times \left[-L_{\tilde{y}}, L_{\tilde{y}}\right]$: with $L_{\tilde{x}} = L_{\tilde{y}} = 20; 40; 80; 160,$ and the fixed domain discretization step *h* = 0.5, the following quantities are presented at the end of the iteration procedure:

- values of the numerical solution $\hat{U}_{i,j}$ at the point: $\tilde{x}_i = 0, \tilde{y}_i = L_{\tilde{y}}$,
- values of μ_U,
- the L_2 norm of the error obtained in the minimization procedure (3.4).

$L_{\tilde{x}} = L_{\tilde{y}}$	$\hat{U}^k_{i,j}$ at $\tilde{x}_i = 0, \tilde{y}_i = L_{\tilde{y}}$	μ_U	$\left\| U_B(\tilde{x}_i, \tilde{y}_j) - \hat{U}^k_{i,j} \right\|_{L_2, \Omega_B}$
20	-2.23e-04	1.9355e-01	4.17e-05
40	-5.65e-05	1.9369e-01	4.42e-06
80	-1.41e-05	1.9378e-01	7.56e-07
160	-3.53e-06	1.9381e-01	7.44e-10

Table 1: Characteristic parameters of the minimization procedure for different computational domains

The results from Table 1 demonstrate that the values of μ_U, shown in the third column, converge as the domain becomes larger. Further, the values of $\hat{U}_{i,j}$ given in the second column of Table 1 decay with a rate of $1/\tilde{r}^2$. The results for μ_W exhibit the same convergence, and are excluded for the sake of simplicity and compactness.

Test 2.

The second test reveals the asymptotic of the numerical solution presented in log-log plots. Pictures in Figure 1 demonstrate important aspects of solution's cross sections on four different grids. The computational domain is kept constant as $[-50,\ 50]\times[-50,\ 50]$ and only the domain discretization step *h* changes, *h* = 0.1; 0.2; 0.4; 0.8.

The first two horizontal pictures in Figure 1 present logarithmic scaled plots of the absolute value of the numerical solution $\hat{U}$. One can see the decay $1/\tilde{r}^2$ at infinity guided by the black line. The next two horizontal pictures show the numerical solution scaled by a factor r^2. Thus these graphs display $\tilde{r}^2\hat{U}$ along the vertical *z* axis. One can observe that for large values of $\tilde{r}$ the scaled profile of the solution approximates a constant. These plots are in agreement with the new boundary function found in (3.3) and with the asymptotic of the solution. Further, using equation (3.3) for *x* = 0 or for *y* = 0, one has for sufficiently large *r* that

$$\tilde{U}(0,\tilde{y}) = -\frac{\mu_U}{\tilde{y}^2}, \quad \tilde{U}(\tilde{x},0) = \frac{\mu_U}{(1-\tilde{c}^2/\beta)\tilde{x}^2}.$$

This fact explains the connection between the two constants (black line) displayed on bottom pictures in Figure 1.

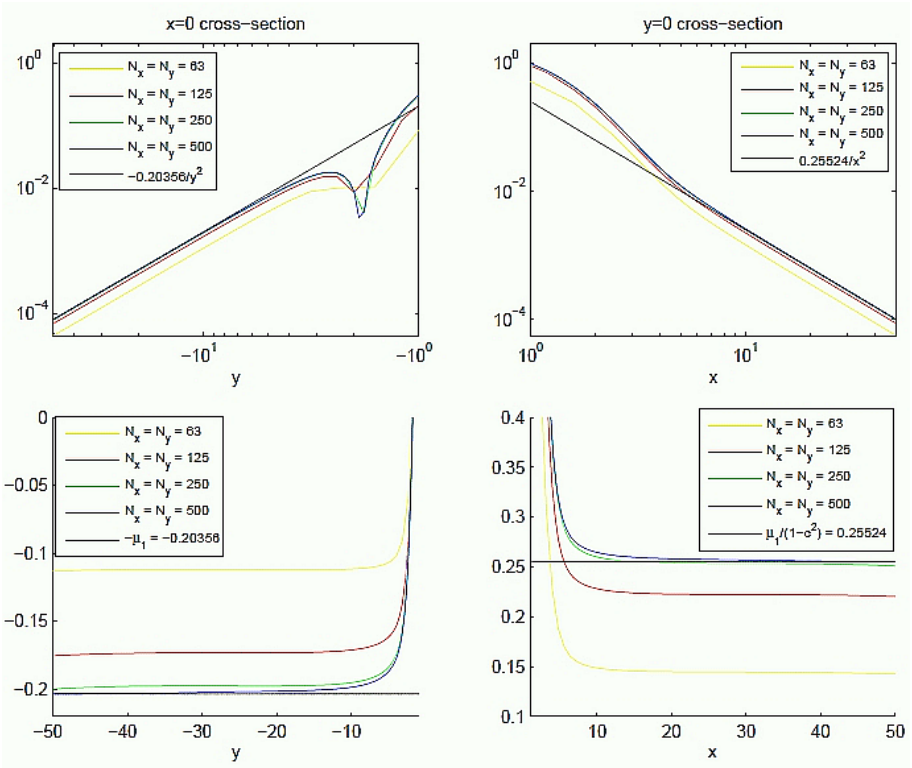

Figure 1. The effect of the mesh size. Upper panels: function $\hat{U}$. Lower panels: $\tilde{r}^2\hat{U}$.

We conclude, that the asymptotic decay of the numerical solution is confirmed with high accuracy.

5. Results and Discussion

On Figure 2 one can see the shape of the solution *U* to elliptic problem (3.2) (equiv. to problem (1.3) in the coordinate system (3.1)) for two combinations of parameters *c* and *β*: *c=0.9, β=1* and *c=0.5, β=3.*

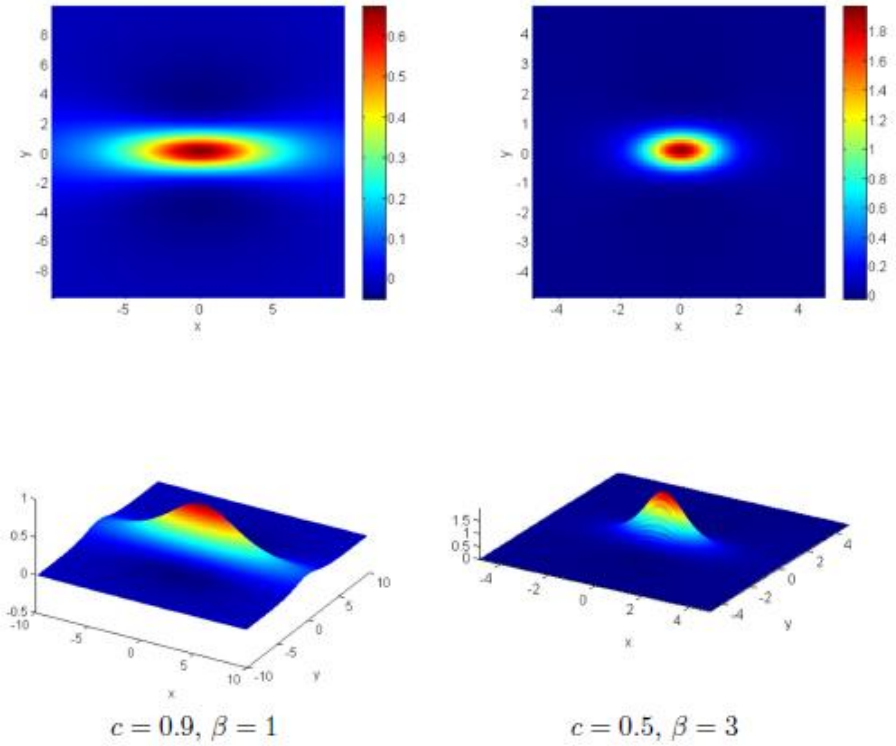

Figure 2. 2D and 3D shapes in the localized domain $[-10,10]\times[-10,10]$.

On Figure 3 we compare the profiles of the numerical solution, obtained in this paper, with the 'best-fit' solution given in [8] and [11], for parameters $c = 0.9, \beta = 1$. In the graphics of both solutions there are sub-domains, where the sign of the numerical solution is negative and the values of the solution are relatively small. These domains are colored in blue.

In the neighborhood of the origin both profiles look very similarly. The main difference between two numerical solutions can be seen near the computational boundary. The domains with negative sign of the solution (so called 'depressions') are different. For the solution, obtained by the method in this paper, this domain depends on the value of the speed *c* since the new boundary function (3.3) satisfies the formulas:

$$U(\tilde{x},\tilde{y})\Big|_{\partial\tilde{\Omega}}\begin{cases}>0, & \text{for } |\tilde{y}|<|\tilde{x}|\sqrt{1-\tilde{c}^2/\beta}\\ <0, & \text{for } |\tilde{y}|>|\tilde{x}|\sqrt{1-\tilde{c}^2/\beta}\end{cases}, \quad (5.1).$$
$$\tan(\phi)=\frac{\tilde{y}}{\tilde{x}}\Big|_{|\tilde{y}|=|\tilde{x}|\sqrt{1-\tilde{c}^2/\beta}}=\pm\sqrt{1-\tilde{c}^2/\beta}.$$

The 'best-fit' solution from [11] obeys the following law:

$$U(\tilde{x},\tilde{y})\Big|_{\partial\tilde{\Omega}}\begin{cases}>0, & \text{for } |\tilde{y}|<|\tilde{x}|\\ <0, & \text{for } |\tilde{y}|>|\tilde{x}|\end{cases}, \tan(\psi)=\frac{\tilde{y}}{\tilde{x}}\Big|_{|\tilde{y}|=|\tilde{x}|}=\pm 1. \quad (5.2)$$

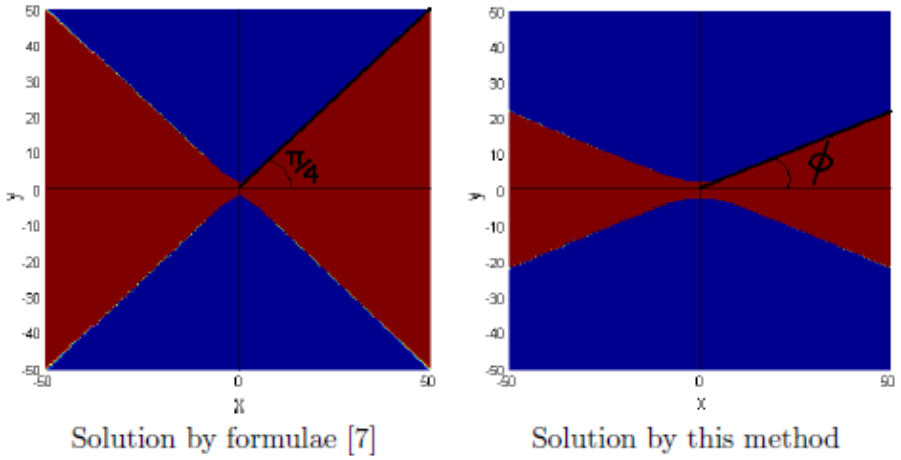

Figure 3. Sign of the solution in the whole domain Ω for $c=0.9, \beta=1$.

The straight black line in Figure 3, where the numerical solution is zero, further validates the asymptotic behavior given by (3.3). The "False Transient Method" used to solve (3.2) corrects the initial condition of the iteration process until it converges to a solution on the inner parts of the domain $\tilde{\Omega}\setminus\partial\tilde{\Omega}$. On the contrary, near $\partial\tilde{\Omega}$, the function is fixed and cannot be corrected.

When the user works with the same coordinate system set, then a difference between the 'best-fit' formulas and the numerical solution $\hat{U}$ on $\partial\tilde{\Omega}$ occurs. The difference is explained by formulas (5.1) and (5.2). Now, the soliton speed $\tilde{c}$ shapes up the boundary condition and the solution is much better modeled near

$\partial\tilde{\Omega}$, especially near the sensitive points $\left\{(\tilde{x},\tilde{y}):|\tilde{y}|=|\tilde{x}|\sqrt{1-\tilde{c}^2/\beta}\right\}$ i.e. when the solution is zero on the boundary.

As an application of the computed here solution to (3.2), the initial energy of the stationary propagating with speed *c* solutions *U* obtained in this paper, is computed in [16]. It is shown there, that for speeds *c>0*.9 this energy is smaller than the potential well depth and, hence, the numerical solution of the nonstationary BE (1.1) with initial data derived in this paper, should not blow up for large time intervals (see [16] for a full explanation).

1.1 Conclusion

In this paper we evaluate the stationary propagating in direction *y* with speed *c* solutions to 2D BE. An iteration method is used to compute the solution of the corresponding fourth order nonlinear elliptic equation. A high order of approximation finite difference scheme is applied for the discretization of spatial derivatives.

We derive a new BC on the boundary of the computational domain. This BC is verified by computation on different grids, different speeds and two dispersion parameters. Near the origin the form of the computed here stationary waves is similar to the presented in [11] form of 'best-fit' stationary solutions, but near the computational boundary both solutions are quite different.

The obtained analytical formulas (2.6), (2.8) and (3.3) of the solution near the boundary give great advantage for the numerical computation of the solutions to stationary BE (1.3) and (3.2) respectively. Instead of choosing a bigger domain to represent the zero boundary conditions at infinity one could use either (2.8) or (3.3).

Results concerning convergence of the iterative method, shape of the solution and a comparison of the numerical solution with the 'best-fit' formula from [11] will be discussed in another article.

The future goal of this paper is to show numerically that equation (1.1) governs the overtaking of wave solution in 2D as shown in the 1D case in [15]. To achieve this a few problems on the boundary have been cleared out. Now, instead of choosing a bigger domain to represent the zero boundary conditions at infinity, one could use either (2.8) or (3.3) as BC.

References

[1] C. I. Christov, An energy-consistent dispersive shallow-water model, Wave Motion, 34, (2001) 161 - 174

[2] Boussinesq, J. (1871). “Theorie de l’intumescence liquide, applelee onde solitaire ou de translation, se propageant dans un canal rectangulaire”. Comptes Rendus de l’Academie des Sciences 72: 755-759
[3] Boussinesq, J. (1872). “Theorie des ondes et des remous qui se propagent le long d’un canal rectangulaire horizontal, en communiquant au liquide contenu dans ce canal des vitesses sensiblement pareilles de la surface au fond”. Journal de Mathematiques Pures et Aplliquees. Deuxieme Serie 17: 55-108
[4] Christov, C.I.: An energy-consistent Galilean-invariant dispersive shallow-water model. Wave Motion 34, 161-174 (2001)
[5] I. Christov, C.I.Christov, Physical dynamics of quasi-particles in nonlinear wave equations, arxiv.org/pdf/nlin/0612005
[6] J. K. Perring, T. H. R. Skyrme, A model unified field equation, Nuclear Physics 31 (1962) 550-555
[7] C. I. Christov, Numerical implementation of the asymptotic boundary conditions for steadily propagating 2D solitons of Boussinesq type equations, Mathematics and Computers in simulation, 82 (2012), 1079-1092
[8] J. Choudhury, C. Christov, 2D Solitary waves of Boussinesq equation, CP75, (2005) 8590
[9] M. Christou, C. I. Christov, Fourier Galerkin method for 2D solitons of Boussinesq equation, Mathematics and Computers in Simulation 74 (2007) 8292
[10] M. Christou, C. I. Christov, Galerkin Spectral Method for the 2D Solitary Waves of Boussinesq Paradigm Equation, CP 1186 (2009) 217 { 225
[11] C. I. Christov, J. Choudhury, Perturbation solution for the 2D Boussinesq equation, Mech. Res. Commun., 38 (2011) 274 { 281
[12] B. Engquist and A. Majda, Absorbing boundary conditions for the numerical simulation of waves, Math. Comp., 31 (1977), pp. 629–651.
[13] C. I. Goldstein, A finite element method for solving Helmholtz type equations in waveguides and other unbounded domains, Math. Comp., 39 (1982), pp. 309–324.
[14] H.Han, W. Bao, Error estimates for the finite element approximation of problems in unbounded domains, SIAM J. NUMER. ANAL. 37, No. 4, pp. 1101–1119
[15] N. Kolkovska, Two Families of Finite Difference Schemes for Multidimensional Boussinesq Paradigm Equation, AIP Conf. Proc. 1301, 395 (2010) http://dx.doi.org/10.1063/1.3526638
[16] N. Kolkovska, K. Angelow, Numerical Computation of the Critical Energy Constant for Two-dimensional Boussinesq Equations, AIP Conf. Proc. 1684, 080007-1–080007-6; doi: 10.1063/1.4934318
[17] P.Northrop, P.A.Ramachandran, W.Schiesser, V. R.Subramanian, A robust false transient method of lines for elliptic partial differential equations, Chemical Engineering Science 90 (2013) 32–39